

Geometry and Kinematics of a Dancing Milky Way: Unveiling the Precession and Inclination Variation across the Galactic Plane via Open Clusters

ZHIHONG HE (何治宏)¹

¹*School of Physics and Astronomy, China West Normal University, No. 1 Shida Road, Nanchong 637002, China*

ABSTRACT

This Letter presents a study of the geometry and motion of the Galactic disk using open clusters in the Gaia era. The findings suggest that the inclination θ_i of the Galactic disk increases gradually from the inner to the outer disk, with a shift in orientation at the Galactocentric radius of approximately 6 ± 1 kpc. Furthermore, this study brings forth the revelation that the mid-plane of the Milky Way may not possess a stationary or fixed position. A plausible explanation is that the inclined orbits of celestial bodies within our Galaxy exhibit a consistent pattern of elliptical shapes, deviating from perfect circularity; however, more observations are needed to confirm this. An analysis of the vertical motion along the Galactocentric radius reveals that the disk has warped with precession, and that the line-of-nodes shifts at different radii, aligning with the results from the classical Cepheids. Although there is uncertainty for precession/peculiar motion in Solar orbit, after considering the uncertainty, the study derives a median value of $\dot{\phi}_{LON} = 6.8 \text{ km s}^{-1} \text{ kpc}^{-1}$ in the Galaxy. This value for the derived precession in the outer disk is lower than those in the literature due to the systematic motion in Solar orbit ($\theta_i = 0.6^\circ$). The study also finds that the inclinational variation of the disk is significant and can cause systematic motion, with the variation rate $\dot{\theta}_i$ decreasing along the Galactic radius with a slope of $-8.9 \mu\text{as yr}^{-1} \text{ kpc}^{-1}$. Moreover, the derived $\dot{\theta}_i$ in Solar orbit is $59.1 \pm 11.2_{\text{sample}} \pm 7.7_{V_{Z\odot}} \mu\text{as yr}^{-1}$, which makes it observable for high precision astrometry. The all-sky open cluster catalog based on Gaia DR3 and Galactic precession/inclinational variation fits as well as Python code related to these fits are available at <https://nadc.china-vo.org/res/r101288/>.

Keywords: Galaxy: stellar content - star clusters: general -Galaxy: warp

1. INTRODUCTION

When observing galaxies, astronomers often find that the disk is bent or tilted (Jarrett et al. 2003) - this is known as the warp structure. It is believed that this phenomenon is caused by a variety of sources of gravitational influence, such as interactions with neighboring galaxies or dark matter halos (e.g. Hunter & Toomre 1969; Sparke & Casertano 1988; Quinn et al. 1993; Shen & Sellwood 2006). The motion of stars and gas in a galaxy's disk can cause distortion in its shape by moving in different directions or orbits. To study the warp structure of galaxies, researchers use observations of the positions and movements of stars and gas clouds (e.g. Sancisi 1976; Bosma 1981; Thilker et al. 2005) along with simulations and models of galactic dynamics (e.g. Pringle 1992; Velazquez & White 1999; Robin et al. 2003; Roškar et al. 2010). A deeper understanding of the warp structure is crucial to comprehend the evolution of galaxies and the underlying processes that drive their formation and transformation in the universe.

The warped structure in the outer disk of our Milky Way has been known for some time, first detected through the observation of HI gas (Kerr 1957; Burke 1957). Studies have shown that the vertical angle increases to 3 degrees at a Galactocentric radius of around 16 kpc (Burton 1988). Similarly, molecular CO clouds observed in the first and second Galactic quadrant have also demonstrated similar warp features in the outer arm (Dame & Thaddeus 2011; Sun et al. 2015). However, the uncertainty of gas kinematic distances has made it difficult to study the geometric structure of the Galactic warp. It was only through the observation of classical Cepheids (Chen et al. 2019; Skowron et al. 2019a, hereafter CCs) in recent years that a clear warp in the outer disk has become measurable. This allowed for the direct measurement of the Galactocentric radius (R_{GC}) and scale height of the warp. Findings indicate that both the gas and young star disk warp upwards in the first and/or second quadrants, and downwards in the third and/or fourth quadrants. Moreover, the absolute vertical amplitude reaches 0.3 to 5 kpc above the Galactic plane beyond

$R_{GC} = 10$ to 30 kpc (e.g. Gum et al. 1960; López-Corredoira et al. 2002; Nakanishi & Sofue 2003; Levine et al. 2006; Voskes & Butler Burton 2006; Chen et al. 2019; Skowron et al. 2019a,b; Lemasle et al. 2022), highlighting the significant dimensions of the warp structure.

Furthermore, the orbital inclination of the warp can lead to a systematic velocity in the vertical direction, particularly close to the line-of-node (LON) where the warp surface intersects with the Galactic plane. During the ascending semicycle, this systematic velocity often displays an upward trend while the opposite is observed in the descending semicycle. Multiple statistical studies have identified this trend using various stellar tracers (López-Corredoira et al. 2014; Liu et al. 2017; Poggio et al. 2017), especially with the improved accuracy of proper motion data from later Gaia releases (Gaia Collaboration et al. 2018, 2021, 2022b). Additionally, the vertical velocity of stars in low-latitude regions near the Galactic plane can be determined by its proper motion μ_b and is less influenced by the radial velocity (e.g. Poggio et al. 2018, 2020; Romero-Gómez et al. 2019; Wang et al. 2020; Li et al. 2020; Cheng et al. 2020; Li et al. 2023; Dehnen et al. 2023).

The question of whether the Milky Way’s warped disk is precessing has sparked debate. Poggio et al. (2020) and Cheng et al. (2020) proposed that there is precession of around 10.9 and 13.6 km s⁻¹ kpc⁻¹ in the outer Galactic disk, respectively, while others argue that there is no significant precession (e.g. Wang et al. 2020; Chrobáková & López-Corredoira 2021). The debate stems from the fact that the precession velocity calculation depends on different tracers and warp models. Recently, Dehnen et al. (2023) introduced a new perspective on precession in the outer disk of the Milky Way based on classical Cepheids, which takes into account the unsteady inclination (known as the inclinational variation rate $\dot{\theta}_i$ in this context) for the first time. This study showed a precession rate that gradually decreases from 12 ($R_{GC} = 12$ kpc) to 6 ($R_{GC} = 14$ kpc) km s⁻¹ kpc⁻¹ without any inclination variations. However, the previously mentioned studies only indicate precession (or lack thereof) in the Galactic outer disk ($R_{GC} > 9$ kpc), without any evidence of warping in the inner Galaxy.

Star clusters are essential in Galactic studies because they provide more precise distance and motion estimates compared to individual stellar tracers. However, only a few open clusters (OCs) located in the southern warp have been identified in previous study (Cantat-Gaudin et al. 2020). This is primarily due to the scarcity of distant OCs, making it difficult to explore the geometry of the Milky Way warp on a larger scale. Recently, we discovered nearly 1500 reliable open clusters through machine learning and visual inspection based on Gaia DR3 (He et al. 2023b). This new result represents a substantial improvement over previous studies, which identified only one-fourth of the present sample’s distant OCs located more than 4 kpc away. This immense dataset presents an opportunity to explore the wider disk via OCs’ study that were previously unattainable. The primary objective of this study is to utilize this extensive sample of Gaia DR3-based OCs to gather vital geometric and kinematic information throughout the Galactic disk. By doing so, it may provide us with further insight into the Milky Way’s warp.

Chapter 2 introduces the selection process and the warp structure inferred from open clusters and classical Cepheids. Chapters 3 and 4 present the geometry and kinematic results, respectively. We analyze how orbital inclination, precession, and inclinational variation changes at different radii. The study presents an in-depth analysis of these findings, providing necessary insights into the warp structure traced by the sample. Chapter 5 summarizes the paper’s main findings and presents potential future research opportunities. Finally, Appendix A presents error analysis of the OC sample, and Appendix B show a sketch map of elliptical inclined plane.

2. OC SAMPLE AND WARP STRUCTURE

Our study utilized a large sample of 2017 open clusters from Cantat-Gaudin et al. (2020), previously used to study the structure of the Milky Way disk within approximately 4 kpc of the Solar system in the Gaia DR2 era. We then cross-matched the member stars of these clusters in Gaia DR3, selecting only clusters with 20 or more member stars (a total of 1837 clusters). Additionally, we obtained new star clusters from Gaia DR2 and EDR3 with a sample size of over 500, including 615 in He et al. (2021, 2022), 628 in Castro-Ginard et al. (2022), and 1656 in He et al. (2023a). We cross-matched the member stars of these clusters in Gaia DR3 to obtain additional line-of-sight velocity information. We removed 138 duplicate clusters (from He et al. 2021, 2022; Castro-Ginard et al. 2022) and 746 clusters with less than 20 member stars (mostly in He et al. 2023a). In total, these clusters contain 3852 open clusters, among which 92% are within 4 kpc. Our study’s sample provides a more extensive dataset for analyzing the structure of the Milky Way’s disk.

Recently, a machine learning algorithm was employed by He et al. (2023b) to identify and verify 2085 star clusters/candidates, out of which 1488 were reliable OCs (Type 1) verified through visual inspection. A total of 944 Type 1 OCs were located beyond 4 kpc, some with large extinction values ($A_V > 5$ mag). Each star cluster underwent isochrone fitting and visual inspection, resulting in a more in-depth analysis of distant OCs’ geometric structure. The coordinates of the above nearby OC samples, combined with Type 1 distant OCs, were transformed into the Galactocentric coordinate system (more details in Appendix A). A significant number of distant star clusters demonstrate the twisted/spiral structures of the Milky Way, as shown in Figure 1.

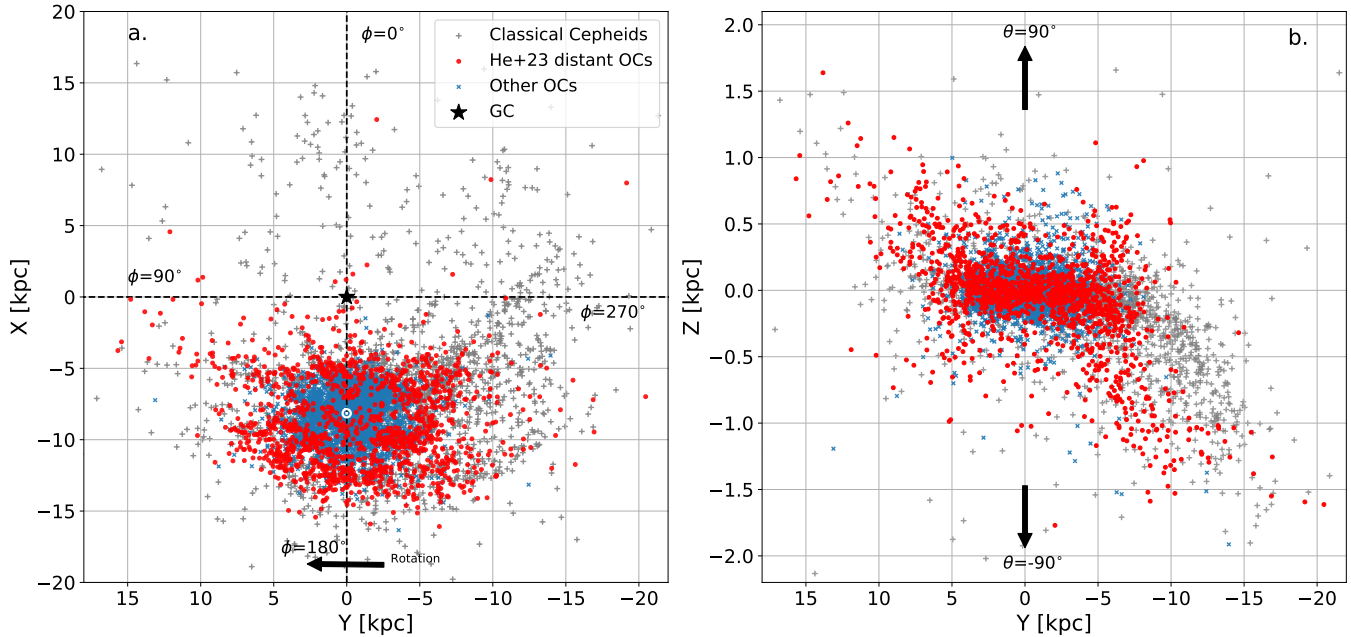


Figure 1. The distribution of open clusters in the XY plane is depicted in both the face-on (a.) and edge-on (b.) views, with Galactocentric coordinates (ϕ, θ) also displayed. In the left panel, the black arrow indicates the rotation direction of the Milky Way, and the position of the Solar system is $(-8.15, 0)$ kpc, according to Reid et al. (2019). Red dots represent distant open clusters from He et al. (2023b), while blue crosses denote other Gaia-based open clusters (Cantat-Gaudin et al. 2020; Castro-Ginard et al. 2022; He et al. 2021, 2022, 2023a). For comparison, the gray pluses signify the CC sample (Skowron et al. 2019a), showing a similar intuitive plot of the warp structure (based on CCs) from Chen et al. (2019); Lemasle et al. (2022); except for the southern warp at $\phi \sim 270^\circ$, which still lack of OC samples there.

This is the second celestial body type, after classical Cepheids (as shown in Figure 1, grey symbols), to directly trace the twisted geometric structure. The highest scale height can reach over 1.5 kpc, both in the southern ($\theta < 0$) and northern ($\theta > 0$) Galaxy. However, the edge-on image from the anti-Galactocentric line shown in Figure 1 only shows the warp in the outer disk. Are there any other tilted or warped structures in the inner regions?

3. DISK INCLINATION

To examine the spatial distribution of open clusters inside and outside the Galactic disk, we present an edge-on view of the plane at different radii using a 2 kpc bin (Figure 2), from the Galactic anticenter direction. The traced disc's degree of tilt by the cluster increases as the radius gets larger, demonstrating that the Milky Way's disc is tilted at various radii. Although the tilt is not very apparent at 6 kpc, a trend of tilt angle change can be observed. Remarkably, the distribution of Cepheid variables exhibits the same tilt pattern, and their distances obtained through the period-luminosity relation indicate consistency with the geometric distribution derived from Gaia's parallax measurements. Our analysis suggests that the tilted disc structure is not unique to outer disk, as previously thought, but rather extends to other regions. Such findings could help to refine our understanding of the Milky Way's structure.

To shed more light on our findings, we categorized the OC samples into three sub-groups based on their age: young (YOCs < 100 Myr), middle-aged (MOCs: 0.1-1 Gyr), and old (OOCs > 1 Gyr) OCs. Interestingly, the inclination angles observed by different age tracers show only slight variations, indicating that YOCs and MOCs are highly consistent. On the other hand, OOCs usually show varying degrees of tilt; however, the trend of the tilt angle change is consistent with the other samples. We attribute this inconsistency among older clusters to radial migration or incomplete sub-samples. As presented in Figure 2, there is a consistent inclination angle of about 0.6 degrees on the orbit where the Sun is located. This value remains consistent for YOCs, MOCs, and CCs, with only a slightly larger inclination in OOCs. However, in the case of older clusters, the member stars in the main sequence exhibit a tendency to be fainter compared to their younger counterparts. This difference in brightness has the potential to result in notable variations in the observed distribution between the older OCs and the younger ones, particularly under heavy extinctions. Consequently, the apparent strong pattern observed in older samples, particularly within the 3 to 5 kpc range of R_{GC} (Figure 2), may not accurately reflect the true inclination.

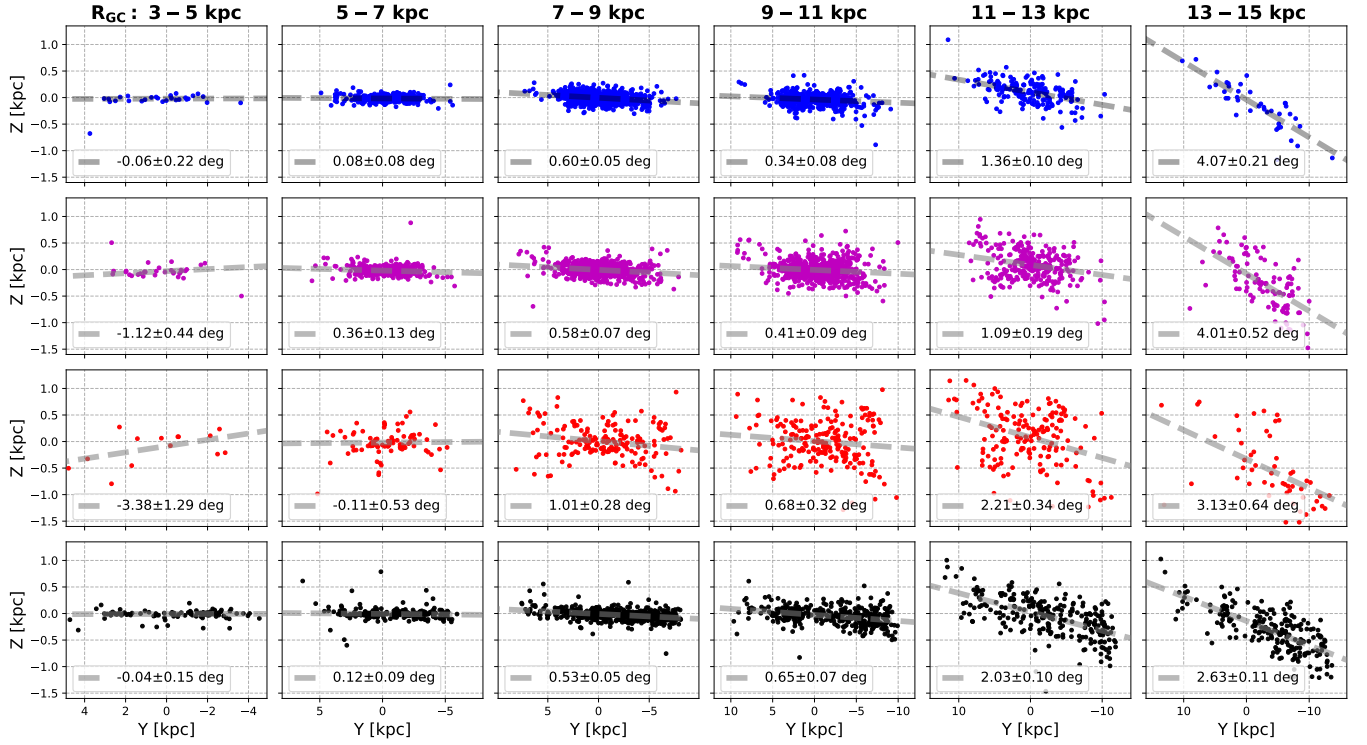


Figure 2. The edge-on views display Gaia-based open clusters (colored dots) and classical Cepheids (black dots) from Skowron et al. (2019a) located at varying Galactocentric radii around $R_{GC} = 4, 6, 8, 10, 12,$ and 14 kpc, all within a width range of ± 1 kpc. The gray dashed line shows the linear regression of the inclination angle on the line of sight anti-Galactic center. Young ($< 10^8$ yr), middle-aged ($10^8 - 10^9$ yr), and old ($> 10^9$ yr) OCs are identified by the blue, magenta, and red symbols, respectively. As the radius increases, the thickness of the OC/CC disks gradually increase, displaying flaring characteristics. Additionally, compared to younger open clusters, the older ones tend to have higher scale heights, as stated in Cantat-Gaudin et al. (2020). It is essential to note that the LON are not situated at $Y = 0$ kpc, and the fitted θ_i is visible in Figure 3-a.

To calculate the Milky Way disc's inclination angle (θ_i) and minimize uncertainties caused by bin selection and LON positions, we fitted OC sample values at different radii using a 0.5 kpc step and obtained the LON position from the OC kinematics (Section 4). During this process, we discovered that the disk did not share a cohesive plane at different radii and that the scale height of the Solar system varied in different literature. Additionally, The lopsided warps were presented in various radius, particularly in the outer arm regions. We believe this is due to the objects' orbits not being circular but instead elliptical (discussed in Section 5). Nevertheless, to simplify our calculation, we used a circular orbit approximation and added d_{Z_0} to eliminate orbital ellipticity/ Z_0 impact on the scale height:

$$Z(R_{GC}, \phi_{GC}, \phi_{LON})_{obs} = R_{GC} \times \sin(\phi_{LON} - \phi_{GC}) \times \sin \theta_i + d_{Z_0} \quad (1)$$

Here, ϕ_{LON} and ϕ_{GC} represent the position of LON and OC samples in Galactocentric coordinates, and Z_{obs} denotes the OCs' scale height. Figure 3-a displays the inclination angle of the disk at different radii, and the error bars reflect the uncertainty in using OC samples of varying age limits. From the inner disk to the outer disk, the tilt angle gradually increases, with the absolute value of the tilt angle being approximately 0° near $R_{GC} = 6$ kpc, and the tilt direction changes. The tilt angle experiences a slight decrease near $R_{GC} = 10$ kpc, followed by a rapid increase to 3 degrees at $R_{GC} = 14$ kpc. Unfortunately, the insufficient OC samples within $R_{GC} = 4$ kpc leaves the orbital tilt in the Milky Way bulge unknown. Nevertheless, the limited information we do have suggests a negative trend in the inclination angle at that location.

The consistent geometric features of tilt disks displayed by different sub-samples, as illustrated in Figure 2 and Figure 3, indicate that the samples utilized in this study are adequately representative for investigating the warp structures, especially for YOCs and MOCs. The degree of tilt at most radii appears to be less reliant on the sample selection. Additionally, as previously stated, orbital tilt is not solely reflected in geometric features; it also displays a vertical systemic velocity in kinematics, which is unaffected by extinction in the Galactic inner disk. As shown in Figure 4, a notable negative value is presented in the vertical velocity in the

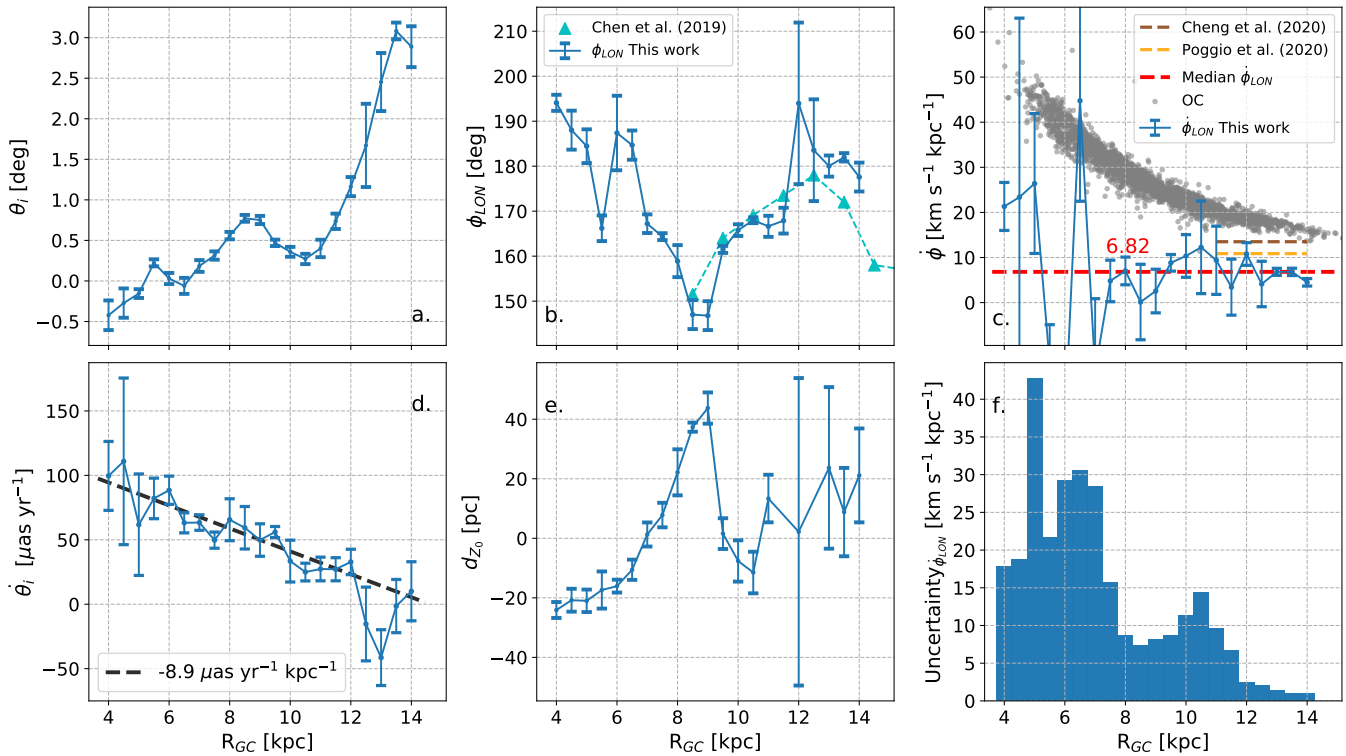


Figure 3. The derived parameters from Equation 1 and 2 are presented with error bars accounting for uncertainties in OC sample age limitations. The parameters include: (a) inclination angle θ_i , (b) LON positions ϕ_{LON} , (c) precession rate $\dot{\phi}_{LON}$, (d) inclinational variation rate $\dot{\theta}_i$, (e) differential scale height d_{z_0} , and (f) uncertainty (from V_\odot) of ϕ_{LON} , plotted against Galactocentric radius R_{GC} . The typical uncertainty resulting from V_\odot for θ_i is $4.3 \mu\text{as yr}^{-1}$.

inner Galactic disc. This value is still maintained despite uncertainties regarding the Sun’s peculiar motion, orbital precession, and inclinational variation in the Galaxy. When combined with their geometric features, these compelling pieces of evidence demonstrate that the orbit of the most inner regions of the Milky Way is also tilted, and the direction of this tilt is opposite to that of the outer disk.

4. GALACTIC MOTION

As mentioned above, a tilted disc can cause a vertical velocity component that reaches its maximum near the LON and gradually decrease towards zero at the highest point of the warp 90 degrees away from the northern/southern solstices. Moreover, a positive LON rotation (precession, $\dot{\phi}_{LON}$) can weaken the $V_{Z\odot}$ systematical velocity caused by this tilted orbit. Figure 4 displays the measured results at $R_{GC} = 13$ kpc, revealing that if only tilt and no precession existed, the observed vertical velocity would be higher. However, the observed velocity is consistent with a precession rate of $\dot{\phi}_{LON} = 6.8 \text{ km s}^{-1} \text{ kpc}^{-1}$, which is lower than what some previous studies (Poggio et al. 2020; Cheng et al. 2020) have reported. Nonetheless, this outcome is independent of any warping or kinematic model, confirming the presence of the precession of the Milky Way.

The Galactic coordinate system exhibits hints of rotation, ranging from 0.05 to 0.8 mas yr^{-1} , based on various objects and observations (e.g. Miyamoto & Zhu 1998; Zhu 2000; Bobylev & Bajkova 2019). Lindegren et al. (2018) identified in Gaia data that the rotation is not more than 0.15 mas yr^{-1} , showing 0.1 mas yr^{-1} when several VLBA sources were compared (Lindegren 2020). Such a magnitude of frame rotation can also affect the proper motion μ_b or vertical velocity in Solar orbit systematically. For instance, a $50 \mu\text{as yr}^{-1}$ rate may cause 0 ($\phi_{LON} = 0^\circ$) to $\sim \pm 2 \text{ km s}^{-1}$ ($\phi_{LON} = \mp 90^\circ$) vertical velocity around the Solar orbit. Additionally, it is reasonable to consider the variation of inclination since the inclination itself needs to increase/decrease to the current positions. Nevertheless, previous investigations on warping disks did not consider its effect, except for recent work Dehnen et al. (2023). In this study, the precession $\dot{\phi}_{LON}$ and mean (since the orbit is not a rigid body) inclinational variation

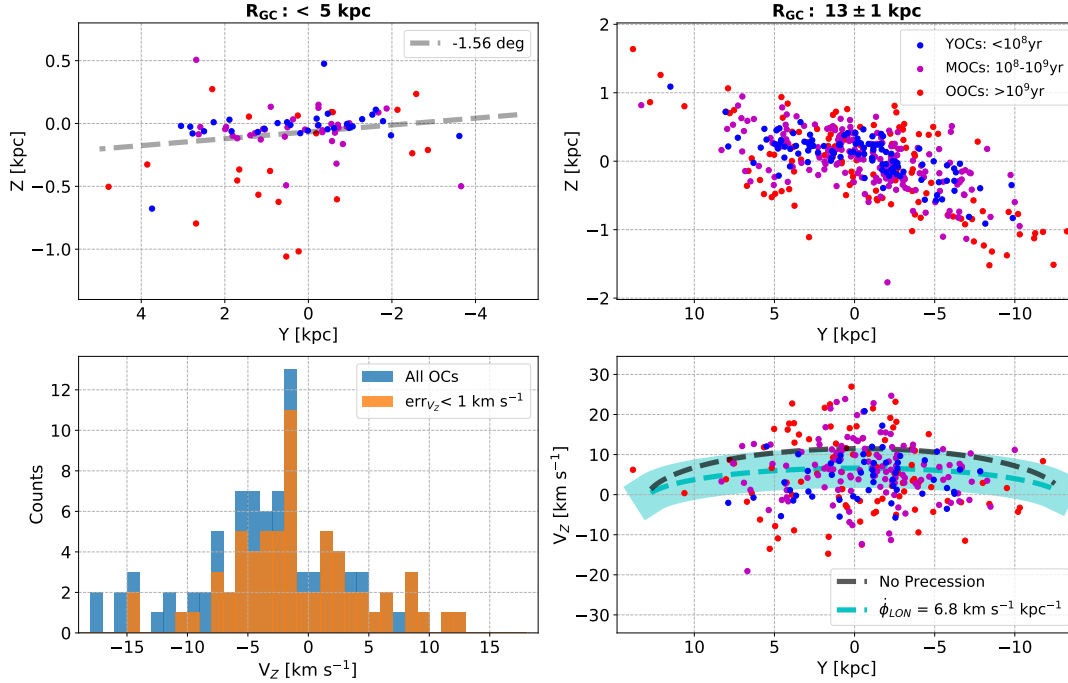


Figure 4. The edge-on views of OCs in the inner (left upper panel) and outer (right upper panel) Galactic disk, along with their corresponding vertical velocity distributions (displayed in the lower panels) are presented. A linear regression is applied (gray dashed line) to demonstrate the smaller inclination angles of the inner disk for clear visualization. Even though the inner disk does not exhibit the same significant tilt as the outer disk, a noticeable negative V_Z is still observed, consistent with the direction of the tilt-induced velocity deviation. In the right lower panel, the black dashed line and cyan dashed line represent the vertical velocity when precession rate $\dot{\phi}_{LON} = 0$ and $6.8 \text{ km s}^{-1} \text{ kpc}^{-1}$, respectively. It can be observed that the $\dot{\phi}_{LON} = 0$ does not correspond to the observed V_Z distribution, as supported by the study conducted by Poggio et al. (2020) utilizing proper motions of giant stars.

$\dot{\theta}_i$ are described by the simple equation:

$$V_Z(R_{GC}, \phi_{GC}, \theta_i)_{obs} = \frac{|\theta_i|}{\theta_i} \times \left(\frac{R_{GC} \times (\dot{\phi}_{GC} - \dot{\phi}_{LON})}{\sqrt{\frac{1 + \tan^2(\theta_i)}{\cos(\phi_{LON} - \phi_{GC})} - 1}} \right) + \dot{\theta}_i \times R_{GC} \times \sin(\phi_{LON} - \phi_{GC}) \times \cos(\theta_i) - V_{Z\odot} \quad (2)$$

The most significant uncertainty when calculating the precession rate is $V_{Z\odot}$ due to the 0.6-degree inclination near the Solar orbit, along with potential uncertainties from Solar peculiar motion, precession, and inclination variation near the Sun. To compensate, an uncertainty of $V_{Z\odot} = 1 \pm 1 \text{ km s}^{-1}$ was added. Using the OC kinematics, LON positions of all radii were fitted, leading to a wide distribution around $\phi = 170^\circ$ (Figure 3-b). The LON positions in the outer Galactic disk ranges from $\phi = 145^\circ$ ($R_{GC} = 8 \text{ kpc}$) to 180° ($R_{GC} = 14 \text{ kpc}$), consistent with the LON positions from CC samples (Chen et al. 2019), whereas the inner regions show an opposite trend. Additionally, our study revealed that the potential systematic movement associated with the rotation of the LON around the line-of-solstice is negligible, with an error bar of approximately $\sim 10 \mu\text{s yr}^{-1}$.

In the inner disk, despite a large sub-sample size, the small absolute value of the tilt angle (especially at $R_{GC} = 5$ to 7 kpc , where the θ_i is close to zero) results in a significant influence of $V_{Z\odot}$ uncertainty on the outcome. A slight change in $V_{Z\odot}$ can cause a large differential $\dot{\phi}_{LON}$ (Figure 3-f). Nevertheless, considering the uncertainty, a precession rate greater than zero ($> 5 \text{ km s}^{-1} \text{ kpc}^{-1}$ or greater) can be observed at $R_{GC} = 4 \text{ kpc}$, indicating the presence of precession characteristics in the inner disk, similar to the outer disk. Figure 3-d shows inclinational variation across the Milky Way disk, where $\dot{\theta}_i$ is higher in the inner disk and decreases with a slope of $-8.9 \mu\text{s yr}^{-1} \text{ kpc}^{-1}$ towards the outer disk. The $\dot{\theta}_i$ in the region where the Solar system is located is $59.1 \pm 11.2_{sample} \pm 7.7_{V_{Z\odot}} \mu\text{s yr}^{-1}$, consistent with hints of previous findings (Lindgren et al. 2018; Bobylev & Bajkova 2019; Lindgren 2020). This inclinational variation across the disk suggests that the rotation of the LON reflects not only the motion of the Solar system but also the interior motion of the entire Galaxy.

5. DISCUSSION AND CONCLUSION

The findings presented in Figure 3-e reveal that the d_{Z_0} values are not zero, suggesting that the median height of the tilted Milky Way disk is not on the same plane. This is likely an indication that the orbital motion of the disk in the Milky Way is a tilted ellipse plane instead of a circular orbit. Upon closer inspection, it was observed that d_{Z_0} steadily increases from $R_{GC} = 4$ to 9 kpc, which could be attributed to the varying position between the two foci at different orbital radii (as depicted in the Sketch map of Appendix B). However, relying solely on ellipse orbit, the observed trend would suggest that eccentricity of the orbits in the inner disk are greater than 0.2 and could even be as high as 0.3, which is not significant enough to serve as evidence. High eccentricity may cause the lopsided warp, but it also give rise to systematic radial motion near the solar orbit. Therefore, it is necessary to conduct further research to gain a more profound understanding of this phenomenon.

This study presents observational evidence for precession and inclinational variation spanning both the inner and outer disks for the first time. The analysis of different-aged OC samples produced significant results, revealing that the precession rates of the Galactic disk are lower than previously reported in the literature. This deviation is attributable to the fact that systematic vertical velocity, which affects the local standard of rest in Solar orbit, has been taken into account. Additionally, a global inclinational variation spread across the Galactic disk may suggest the disk galaxy is presently undergoing a shift in inclination. However, further observations and simulations are necessary to examine its origin better. It should be noted that the considerable rotation of the Solar orbit may impact high precision astrometry, necessitating additional analysis to identify any potential effects of precession and inclinational variation on the coordinate system.

6. ACKNOWLEDGEMENTS

This work has made use of data from the European Space Agency (ESA) mission GAIA (<https://www.cosmos.esa.int/gaia>), processed by the GAIA Data Processing and Analysis Consortium (DPAC, <https://www.cosmos.esa.int/web/gaia/dpac/consortium>). Funding for the DPAC has been provided by national institutions, in particular the institutions participating in the GAIA Multilateral Agreement. This work is supported by "Young Data Scientists" project of the National Astronomical Data Center, CAS (NADC2023YDS-07); and Fundamental Research Funds of China West Normal University (CWNU, No.21E030).

APPENDIX

A. DATA PROCESSING AND ERROR ANALYSIS

We employed the Gaia DR3 data to derive the cluster position and velocity components from the member stars of 5340 open clusters. To do so, we first calculated the weighted means of the member stars' parameters and then adjusted the parallax by adding 0.017 mas (parallax zero point, [Lindegren et al. 2021](#); [Fabricius et al. 2021](#)). By considering the Solar system's position: [$R_{GC\odot}$, Z_{\odot}] are [8.15 kpc, 5.5 pc], and Solar peculiar motion: [U_{\odot} , V_{\odot} , W_{\odot}] are [10.6, 10.7, 7.6] km s⁻¹, and $V_{\phi 0} = 236$ km s⁻¹ ([Reid et al. 2019](#)), we transformed these values into a coordinate system centered on the Galactic center (R_{GC} , ϕ , Z) and a three-dimensional velocity ($V_{R_{GC}}$, V_{ϕ} , V_Z). It is worth noting that 1269 of the 5340 clusters did not have radial velocities, and we estimated the median value by selecting OCs in ($l \pm 10^\circ$, $b \pm 5^\circ$, $\varpi \pm 0.05$ mas) and set the error to maximum of 50 km s⁻¹ and velocity dispersion of the sample.

It is worth mentioning that the uncertainty of the vertical velocity component V_{\odot} had the most substantial impact on our results. Given the variation in W_{\odot} values across different studies (e.g., 7.6, 8.6, and 6.9 km s⁻¹ from VLBA observations, Gaia data, and others, respectively. [Reid et al. 2019](#); [Gaia Collaboration et al. 2022a](#); [Semczuk et al. 2023](#)), we included the effect of this uncertainty in our calculation (Section 4). Furthermore, we added d_{Z_0} to reduce the impact of the inclinational ecliptic orbit and scale height uncertainty in the Solar system (Section 3). To fit for parameters in Figure 3, we selected an open cluster sample with $err_{V_Z} < 1$ km s⁻¹ and $err_{V_{\phi}} < 2.5$ km s⁻¹, which is equivalent to the typical intrinsic velocity dispersion of OCs (around 1 km s⁻¹ or less, [Mermilliod et al. 2009](#)), without placing any distance-based constraints. However, we accounted for distance errors while estimating velocity errors, resulting in the exclusion of some star clusters with large distance errors in the velocity selections. Furthermore, we employed a bin size of 2 kpc while fitting the data, effectively minimizing the effects of distance errors (distance error < 500 pc for 93% of the clusters). Figure 5 depicts the histograms of the derived velocity errors.

B. SKETCH MAP OF ELLIPTICAL INCLINED GALACTIC PLANE

Figure 6 depicts the sketch map of the scale height in the elliptical inclined galactic plane. The corresponding median scale height follows the trend of d_{Z_0} in $R_{GC} = 4$ to 11 kpc, as seen in Figure 3-e.

REFERENCES

- Bobylev, V. V., & Bajkova, A. T. 2019, *Astronomy Letters*, 45, 208
- Bosma, A. 1981, *AJ*, 86, 1791

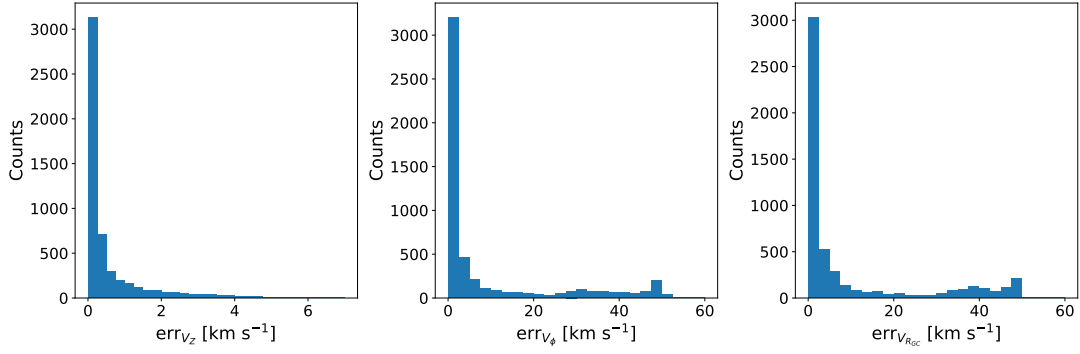


Figure 5. Statistical distribution of velocity component errors presented in the Galactocentric coordinate system, using 1 km s^{-1} bin size for V_z and 2.5 km s^{-1} bin size for V_ϕ and V_{RGC} .

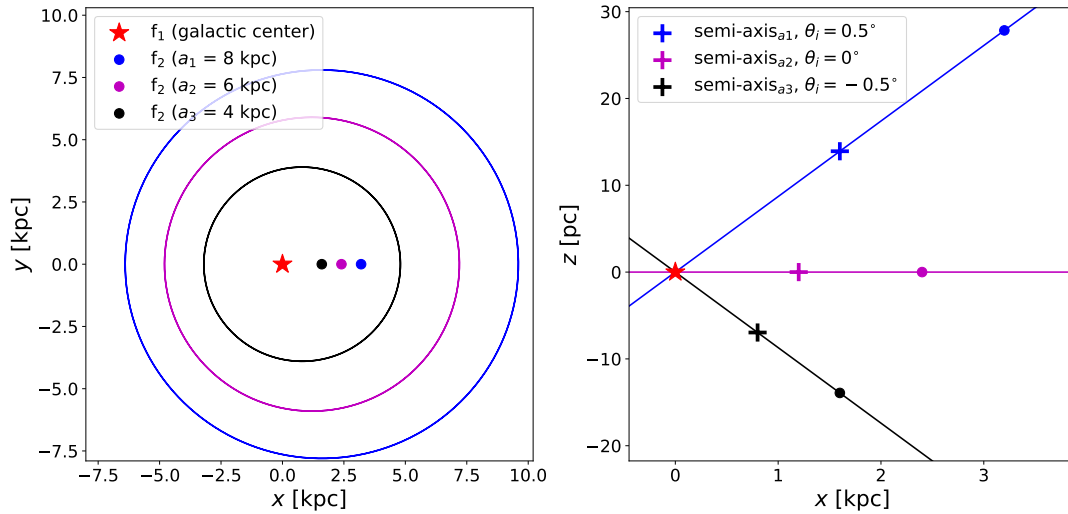


Figure 6. Sketch map of scale height in the elliptical inclined galactic plane. The left panel displays the elliptical plane at different semi-major axis, represented by the function: $x^2/a^2 + y^2/b^2 = 1$, where f_1 (galactic center) and f_2 are the foci, and the eccentricity is set to 0.2. Right panel demonstrates the differential scale height of the f_2 and semi-minor axis, with the inclination angles (θ_i) set at 0.5 (blue), 0 (magenta), and -0.5 (black) degrees.

Burke, B. F. 1957, *AJ*, 62, 90

Burton, W. B. 1988, in *Galactic and Extragalactic Radio Astronomy*, ed. K. I. Kellermann & G. L. Verschuur, 295–358

Cantat-Gaudin, T., Anders, F., Castro-Ginard, A., et al. 2020, *A&A*, 640, A1

Castro-Ginard, A., Jordi, C., Luri, X., et al. 2022, *A&A*, 661, A118

Chen, X., Wang, S., Deng, L., et al. 2019, *Nature Astronomy*, 3, 320

Cheng, X., Anguiano, B., Majewski, S. R., et al. 2020, *ApJ*, 905, 49

Chrobáková, Ž., & López-Corredoira, M. 2021, *ApJ*, 912, 130

Dame, T. M., & Thaddeus, P. 2011, *ApJ*, 734, L24

Dehnen, W., Semczuk, M., & Schönrich, R. 2023, *MNRAS*, arXiv:2305.09343

Fabricius, C., Luri, X., Arenou, F., et al. 2021, *A&A*, 649, A5

Gaia Collaboration, Brown, A. G. A., Vallenari, A., et al. 2018, *A&A*, 616, A1

—, 2021, *A&A*, 649, A1

Gaia Collaboration, Drimmel, R., Romero-Gomez, M., et al. 2022a, arXiv e-prints, arXiv:2206.06207

Gaia Collaboration, Vallenari, A., Brown, A. G. A., et al. 2022b, arXiv e-prints, arXiv:2208.00211

Gum, C. S., Kerr, F. J., & Westerhout, G. 1960, *MNRAS*, 121, 132

He, Z., Liu, X., Luo, Y., Wang, K., & Jiang, Q. 2023a, *ApJS*, 264, 8

He, Z., Luo, Y., Wang, K., et al. 2023b, arXiv e-prints, arXiv:2305.10269

He, Z., Li, C., Zhong, J., et al. 2022, *ApJS*, 260, 8

He, Z.-H., Xu, Y., Hao, C.-J., Wu, Z.-Y., & Li, J.-J. 2021, *Research in Astronomy and Astrophysics*, 21, 093

Hunter, C., & Toomre, A. 1969, *ApJ*, 155, 747

Jarrett, T. H., Chester, T., Cutri, R., Schneider, S. E., & Huchra, J. P. 2003, *AJ*, 125, 525

- Kerr, F. J. 1957, *AJ*, 62, 93
- Lemasle, B., Lala, H. N., Kovtyukh, V., et al. 2022, *A&A*, 668, A40
- Levine, E. S., Blitz, L., & Heiles, C. 2006, *ApJ*, 643, 881
- Li, X., Wang, H.-F., Luo, Y.-P., et al. 2023, *ApJ*, 943, 88
- Li, X. Y., Huang, Y., Chen, B. Q., et al. 2020, *ApJ*, 901, 56
- Lindegren, L. 2020, *A&A*, 633, A1
- Lindegren, L., Hernández, J., Bombrun, A., et al. 2018, *A&A*, 616, A2
- Lindegren, L., Bastian, U., Biermann, M., et al. 2021, *A&A*, 649, A4
- Liu, C., Tian, H.-J., & Wan, J.-C. 2017, in *Formation and Evolution of Galaxy Outskirts*, ed. A. Gil de Paz, J. H. Knapen, & J. C. Lee, Vol. 321, 6–9
- López-Corredoira, M., Abedi, H., Garzón, F., & Figueras, F. 2014, *A&A*, 572, A101
- López-Corredoira, M., Cabrera-Lavers, A., Garzón, F., & Hammersley, P. L. 2002, *A&A*, 394, 883
- Mermilliod, J. C., Mayor, M., & Udry, S. 2009, *A&A*, 498, 949
- Miyamoto, M., & Zhu, Z. 1998, *AJ*, 115, 1483
- Nakanishi, H., & Sofue, Y. 2003, *PASJ*, 55, 191
- Poggio, E., Drimmel, R., Andrae, R., et al. 2020, *Nature Astronomy*, 4, 590
- Poggio, E., Drimmel, R., Smart, R. L., Spagna, A., & Lattanzi, M. G. 2017, *A&A*, 601, A115
- Poggio, E., Drimmel, R., Lattanzi, M. G., et al. 2018, *MNRAS*, 481, L21
- Pringle, J. E. 1992, *MNRAS*, 258, 811
- Quinn, P. J., Hernquist, L., & Fullagar, D. P. 1993, *ApJ*, 403, 74
- Reid, M. J., Menten, K. M., Brunthaler, A., et al. 2019, *ApJ*, 885, 131
- Robin, A. C., Reylé, C., Derrière, S., & Picaud, S. 2003, *A&A*, 409, 523
- Romero-Gómez, M., Mateu, C., Aguilar, L., Figueras, F., & Castro-Ginard, A. 2019, *A&A*, 627, A150
- Roškar, R., Debattista, V. P., Brooks, A. M., et al. 2010, *MNRAS*, 408, 783
- Sancisi, R. 1976, *A&A*, 53, 159
- Semczuk, M., Dehnen, W., Schönrich, R., & Athanassoula, E. 2023, *MNRAS*, 519, 902
- Shen, J., & Sellwood, J. A. 2006, *MNRAS*, 370, 2
- Skowron, D. M., Skowron, J., Mróz, P., et al. 2019a, *Science*, 365, 478
- . 2019b, *Acta Astron.*, 69, 305
- Sparke, L. S., & Casertano, S. 1988, *MNRAS*, 234, 873
- Sun, Y., Xu, Y., Yang, J., et al. 2015, *ApJ*, 798, L27
- Thilker, D. A., Bianchi, L., Boissier, S., et al. 2005, *ApJ*, 619, L79
- Velazquez, H., & White, S. D. M. 1999, *MNRAS*, 304, 254
- Voskes, T., & Butler Burton, W. 2006, arXiv e-prints, astro
- Wang, H. F., López-Corredoira, M., Huang, Y., et al. 2020, *ApJ*, 897, 119
- Zhu, Z. 2000, *Ap&SS*, 271, 353